Journal of Fluorescence (2019) 29:531–540
https://doi.org/10.1007/s10895-019-02366-4

ORIGINAL ARTICLE

Effect of Environment on Protoporphyrin IX: Absorbance, Fluorescence and Nonlinear Optical Properties

Mehdi Hoseini [1] · Ameneh Sazgarnia [1] · Soheil Sharifi [2]

Received: 12 December 2018 / Accepted: 10 March 2019 / Published online: 20 March 2019

Abstract

The present study investiaged the enhancement of nonlinear optical properties of Protoporphyrin IX in photodynamic therapy using nano-droplet. To this end; absorbance, fluorescence, and nonlinear optical properties of Protoporphyrin IX were examined and results showed that dye aggregation and dielectric constant of solvent could change absorbance and fluorescence spectra. According to quantum mechanical perturbation theory, dipole moment of Protoporphyrin IX in solutions of water-ethanol was extracted. The values of nonlinear absorption and nonlinear refractive index of Protoporphyrin IX in AOT/Toluene/H_2O were also reproted to be larger than aqueous solutions, due to polarity reduction of solvent as well as discount of Protoporphyrin IX aggregation in AOT/Toluene/H_2O. Furthermore, the effect of cell culture media on the nonlinear optical properties of Protoporphyrin IX was analyzed and the results were compared with those of water. The photon correlation spectroscopy of solution also showed a growth in dye-droplet aggregation following the increase of Protoporphyrin IX concentration.

Keywords Protoporphyrin IX · PRMI · Microemulsion · Nonlinear optic · Fluorescence · Cell cultural medium · Photon correlation spectroscopy

Introduction

Two-photon photodynamic therapy (TP-PDT) is known as a method to use two photon absorption in Photodynamic Therapy(PDT) [1–3] and also as a way to produce singlet oxygen to destroy cancer tissues [4].

Related studies in this domain have reported that the protoporphyrin IX (PpIX) can be used to examine excitation (TPE) fluorescence microscopy of 5-aminolevulinic acid (5-ALA)-induced production in human glioma spheroids [5]. PpIX is also recognized as one of the most common porphyrins in nature and also an iron-free form of hemin [6]. Moreover, the molecular structure of PpIX can have a large hydrophobic surface with two peripheral ionizable propionate groups. These types of molecules can be also predicted to create dimers or supermolecular structures formed by hydrogen-bonding.

✉ Soheil Sharifi
ssharifi@ferdowsi.um.ac.ir; soheil.sharifi@gmail.com

[1] Department of Medical Physics, School of Medicine, Mashhad University of Medical Science, Mashhad, Iran

[2] Department of Physics, Faculty of Science, Ferdowsi University of Mashhad, Mashhad, Iran

PpIX aggregation in aqueous solutions can be studied via spectrophotometer, fluorimeter, and dynamic light scattering [5]. It has been observed that absorption spectra have a peak at 406 nm at low pH (pH = 1). In an intermediate pH (3 < pH < 7), a broad absorption peak can be also observed with maxima at 352 and 450 nm; and in a higher pH (pH = 12), a peak can be seen at 382 nm. The fluorescence intensity can also have a redshift as pH increases.

It is well known that PpIX is a monomer in the low pH, a dimer form in pH > 8, and a greater aggregation appearing in intermediate pH range of 3–7. So, it can be conlcuded that dye aggregation depends on pH range.

In previous studies, diode-pumped Nd:YVO4 continuous wave laser (532 nm) had been used to study of the two-photon excited fluorescence of PpIX in ethanol and micelle [5] and it had been reported that the two-photon fluorescence rate of PpIX was similar to those for one-photon excitation (OPE). The absorption coefficient (α) could be specified by Eq. 1 [8, 9]:

$$\alpha = \alpha_0 + \beta I \tag{1}$$

Where I is the intensity of laser beam, α_0 shows the linear absorption, and β stands for nonlinear absorption coefficient. The enhancement of nonlinear absorption is also considered

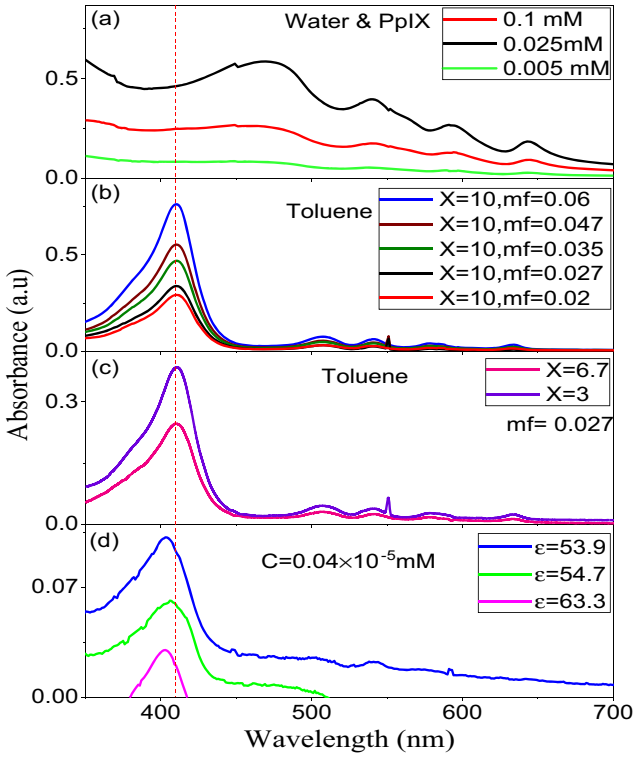

Fig. 1 The absorbance of PpIX in (**a**) water (**b**) AOT/Toluene/H_2O at X = 10 and change of mf, (**c**) AOT/Toluene/H_2O at X = 3 and 6.7 at constant mf = 0.027 with PpIX/Water = 0 .5mM, (**d**) the mixture of water in Ethanol at different dielectric constant of solutions with PpIX/Water = 0.04×10^{-5} mM

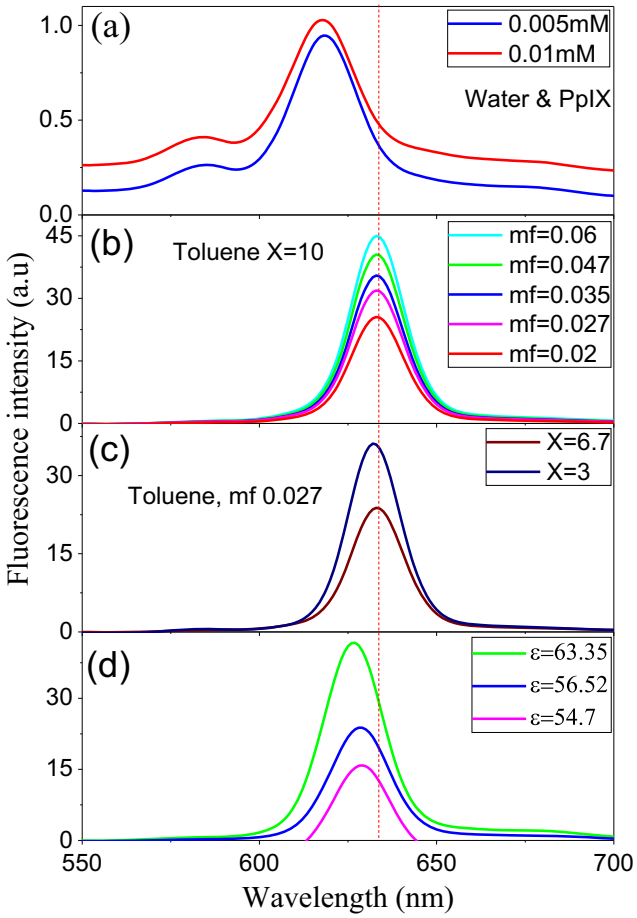

Fig. 2 The absorbance of PpIX in (**a**) water (**b**) AOT/Toluene/H_2O at X = 10 and change of mf, (**c**) AOT/Toluene/H_2O at X = 3 and 6.7 at constant mf = 0.027 with PpIX/Water = 0 .5mM, (**d**) the mixture of water in Ethanol at the different dielectric constant of solutions with PpIX/Water = 0.04×10^{-5} mM

as one of the interesting topics in optics which can have applications in PDT [10].

Moreover, z-scan is a method to study properties of materials [11, 12]. Therefore, z-scan instruments have open and closed apertures and open aperture curve can be specified using Eq. 2 [13, 14]:

$$T_{OA} = \sum_{n=0} (-q_0)^n (n+1)^{-1.5} \tag{2}$$

In which, q_0 is;

$$q_0 = \beta I_0 L_{eff} \left(1 + \left(z.z_0^{-1}\right)^2\right)^{-1} \tag{3}$$

Where L_{eff} is the effective thickness and z_0 represents the Rayleigh length. The intensity also depended on the refractive index (n) which could be described through Eq. 4 [15].

$$n = n_0 + n_2 I \tag{4}$$

In which, n_0 is the linear absorption and the n_2 can be defined by Eq. 5:

$$n_2 = 2\pi I_0 (1 - \exp(-\alpha_0 l))(\Delta\Phi_0 \alpha_0 \lambda)^{-1} \tag{5}$$

Wherein; λ is the wavelength, l indicates cell thickness, and $\Delta\varphi_0$ is the phase. The differences between the peak and the valley of the closed aperture curve could be given as follows:

$$\Delta T_{P-V} = 0.406(1-s)^{0.25} \Delta\varphi_0 \tag{6}$$

In this study, the enhancement of NLO properties of PpIX was studied using a nano-droplet. Moreover, charge effects on the NLO properties of PpIX were examined to understand the enhancement mechanism as well as the impact of polarity on media. For this reason, the NLO properties of the PpIX were investigated by a spectrophotometer, a fluorimeter, and a z-scan instrument. The effect of medium polarity was further examined via changing the solvent from water to water-ethanol and the impact of electrostatic interaction was studied using two types of surfactants. In addition, the effect of AOT/Toluene/H_2O on PpIX was investigated. It should be noted that is studied. The AOT/Toluene/H_2O is a water to oil microemulsion. In this study, the influence of droplet size on NLO properties of PpIX was also investigated. The results revealed that the NLO

Table 1 Shows $\nu a + \nu b(cm^{-1})$,$\nu a - \nu b(cm^{-1})$, ratio of dipole moments $\mu_e\mu_e/\mu_g\mu_g$, the wavelength of the absorption peak $\lambda_{abs,}$ and the fluorescence peak λ_{em} of Azophloxine (PpIX) in organic solvent

Solvent	ε	n	C_{dye} (mM)	λ_{abs} (nm)	λ_{em} (nm)	$\nu_a - \nu_f$ (cm^{-1})	$\nu_a + \nu_f$ (cm^{-1})	$\frac{\mu_e}{\mu_g}$
Water & Ethanol	53.9	1.33	0.04e-3	403	627	8865	40,763	1.45153
Water & Ethanol	54.7	1.33	0.04e-3	407	627	8621	40,519	1.45153
Water & Ethanol	63.3	1.33	0.04e-3	402	626	8902	40,850	1.45153
Water	80	1.33	0.5	403	635	9066	40,562	1.45153

properties of PpIX had changed through the polarity, charge interaction, as well as microemulsion droplet.

Experiment

Materials and Sample Preparation

PpIX; as disodium salt, sodium bis (2-ethylhexyl) sulfosuccinate (AOT), toluene with purities of 99%, and RPMI 1640 medium were bought from Sigma-Aldrich Co. (Munich, Germany). De-ionized water was also used for the preparation of the PpIX solution.

Four types of samples were prepared for this experiment. Firstly, PpIX was assorted through water at 0.5 mM (different) concentration (C_{PpIX}) as a stock. Secondly, PpIX was mixed with droplets. The mixture of the aqueous solution of PpIX in the mixture of AOT in oil with two surfactant to water molar ratio was X = [H_2O]/[AOT], X = 5, and 10. Mass fraction was also considered as droplet mass ratio to total mass (mf = ($m_w + m_{AOT}$)/m_T), wherever $m_T = m_w + m_{AOT} + m_{oil}$), in which m_w is the mass of water, m_{AOT} stands for the mass of AOT, and m_T shows the total mass. Thirdly, the mixture of water with ethanol whose dielectric constant of solutions could change after the increase in ethanol percentage into water and finally, the effect of RPMI concentration on nonlinear optical properties of PpIX doped droplet were studied and the RPMI concentration in solution was described by the mass of dye to the total mass (Y).

Methodology

In this study, the z-scan technique had two types of aperture; closed and open, to find the n_2 and β, separately. In the z-scan instrument, laser (λ = 532 nm, Power = 80 mW) with Gaussian beam was used which was focused through a 5 .0cm lens in which the beam (ω_0) was 1 .1mm and the length of Rayleigh (z_0) was 1 .4μm. The z-scan was prepared in Pars-Optic Co. (Iran).

Absorbance and fluorescence spectra of PpIX in the samples were recorded using a UV-1650 PC spectrometer (Labomed Co., Los Angeles, USA) and a Jasco FP-6200 spectrofluorimeter (Jasco, Japan). PCS measurements were also performed on the samples using Malvern Instruments (Malvern Co., England) with HeNe-laser (632.8 nm) to determine the size of AOT/Toluene/H_2O with and without PpIX.

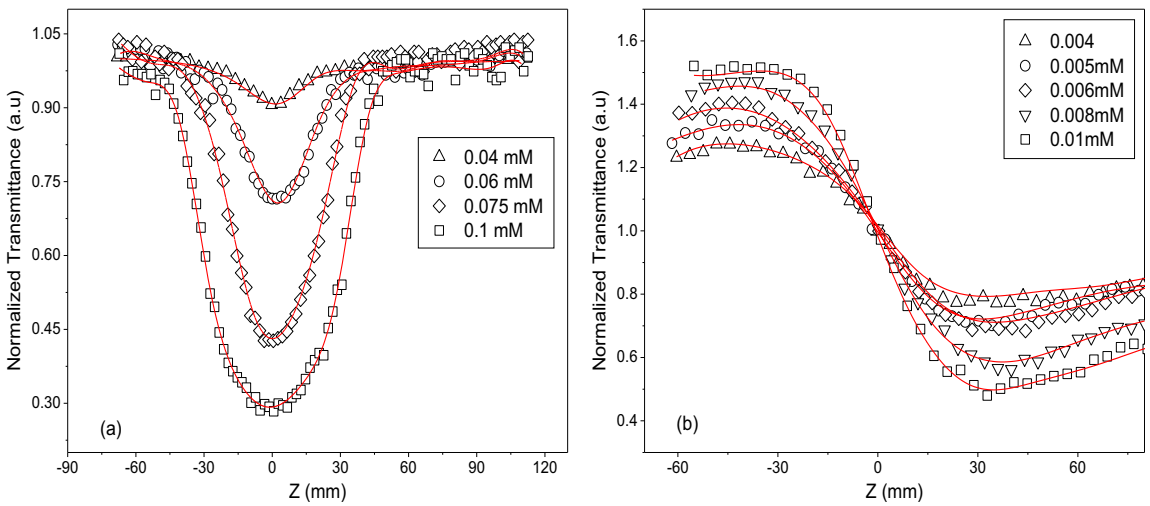

Fig. 3 The normalized (**a**) open and (**b**) close aperture curves of PpIX in water at different dye concentration

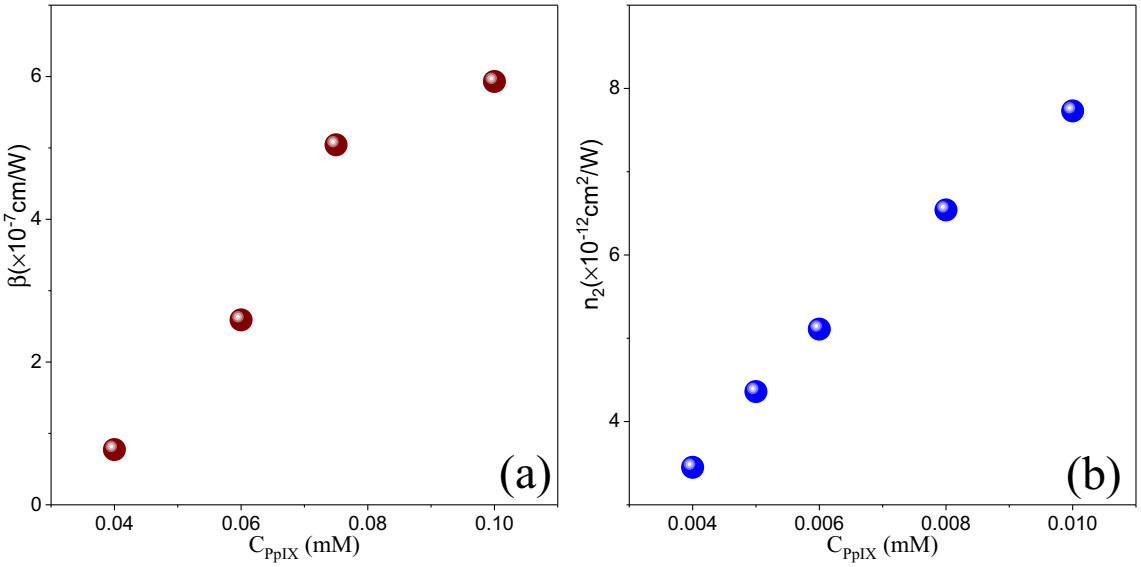

Fig. 4 **a** The nonlinear absorption (β) and **b** nonlinear refractive index (n_2) of PpIX in water as function of dye concentration

Results and Discussion

Photophysics of PpIX in Water and Microemulsion

In this study, the effect of different media on absorbance and fluorescence of PpIX was studied using spectrophotometer and fluorometer. For this purpose, the mixture of PpIX with water, microemulsion, as well as the mixture of water with ethanol were investigated. The absorbance of PpIX in water showed four broad peaks (472, 541, 592, 644 nm) whose wavelengths did not change as PpIX concentration increased (Fig. 1a). A great blueshift in absorbance was also observed through changing the solvent from water to AOT/Toluene/H_2O (Fig. 1b). The results demonstrated that the wavelength

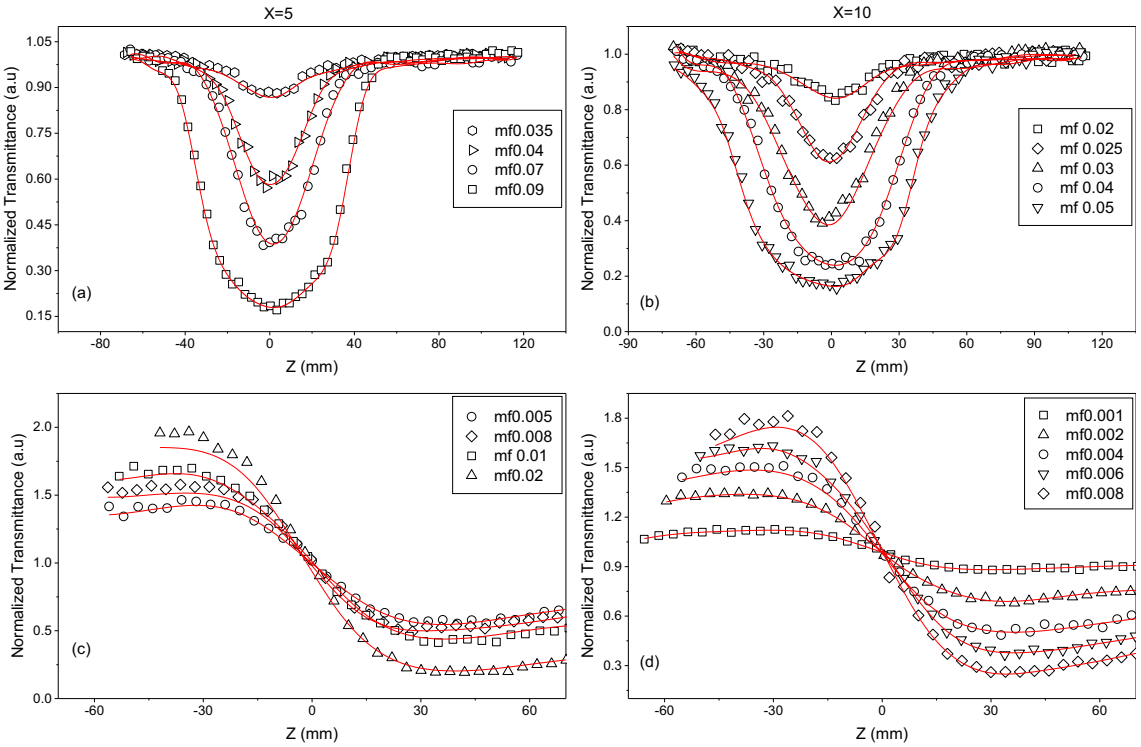

Fig. 5 The open aperture curve of AOT/Toluene/H_2O/PpIX at (**a**) X = 5 and (**b**) X = 10 for the different mass fraction and the close aperture curves of AOT/Toluene/H_2O/PpIX at(c) X = 5, and (d) X = 10 for the different mass fraction, the PpIX/Water = 0 .5mM

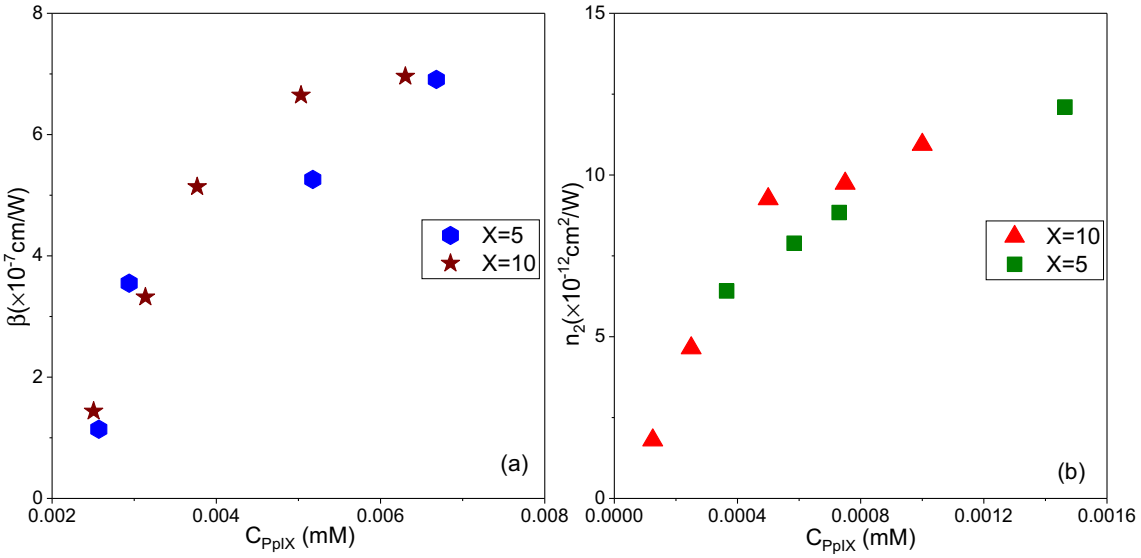

Fig. 6 The value of (**a**) β and (**b**) n_2 of AOT/Toluene/H_2O/PpIX at X = 5 and 10, PpIX/Water = 0 .5mM as a function of PpIX concentration in microemulsion

of peaks had not changed following the increase of droplet mass fraction from 0.02 to 0.06 and the molar ratio from 3 to 10 (Fig. 1b, c).

The absorbance of PpIX in the mixture of water in ethanol was also studied at different concentrations and the absorbance at different dielectric constant (ε) of water in ethanol was presented in Fig. 1d. The reduction of PpIX aggregation after the change of solvent from water to AOT/Toluene/H_2O could describe the redshift of PpIX in the solvents. According to Fig. 1 (d), the wavelength of absorbance peak was not sensitive to the variation of ε.

Moreover, the aggregation of PpIX in aqueous solution was investigated by means of UV-vis spectroscopy [7] and it was observed that the aggregation of PpIX in aqueous solution had a formation similar to multilamellar or onion-like vesicles. It could be proposed that the aggregation of PpIX in microemulsion was less than water, explaining the redshift in absorbance spectra. The fluorescence spectra of PpIX in water at different dye concentrations (Fig. 2a) and in AOT/Toluene/H_2O at two molar ratios (X = 3,6.7,10) (Fig. 2b, c) were correspondingly studied. The fluorescence intensity of PpIX in aqueous solutions displayed a peak at 618 nm wherein the redshift was detected by the change of solvent from water to AOT/Toluene/H_2O (Fig. 2a, b), caused by a decrease of PpIX aggregation. In addition, the redshift of fluorescence depended on the dielectric constant of the solvent (Fig. 2d). The redshift was also distinguished by an increase of dielectric constant of solvents. According to Fig. 2a, b, the fluorescence of PpIX in microemulsion was greater than water solution due to the reduction of dye aggregation in AOT/Toluene/H_2O. The main point was that the fluorescence spectra of X = 3 was higher than other Xs. It means, lower droplet size had greater fluorescence spectra.

In this study, quantum mechanical perturbation theory was utilized to study dipole moment of PpIX in the solution. In this theory, wavenumber of absorption (ν_a) and wavenumber of fluorescence (ν_b) in the component could be labeled by [16, 17, 19]:

$$\nu_a - \nu_b = p_{1\times}\, f + \text{const} \tag{7}$$

$$\nu_a + \nu_b = -p_{2\times}\,(f + 2g) + \text{const} \tag{8}$$

Within these equations, f and g were obtained as follows:

$$f = \frac{2n^2+1}{n^2+2}\left[\frac{\varepsilon-1}{\varepsilon+2} - \frac{n^2-1}{n^2+2}\right] \tag{9}$$

Table 2 The values of χ_R and γ_R of PpIX in water at different dye concentration

Solvent	C_{dye} (mM)	$n_2(\times10^{-12}\ m^2\ W^{-1})$	$X_R^{(3)}(m^3\ W^{-1}\ s^{-1})$	$\gamma_R(\times10^{-20}\ m^6W^{-1}s^{-1})$
Water	0.004	3.45	23.43439	0.390543
	0.005	4.36	29.61563	0.394845
	0.006	5.11	34.71006	0.385638
	0.008	6.5452	44.45877	0.370462
	0.01	7.73	52.50661	0.350017

Table 3 The values of χ_R and γ_R of PpIX in AOT/Toluene/H_2O at X = 5 and 10 with PpIX/Water = 0 .5mM and different droplet mass fraction (mf)

Oil	PpIX/water ratios (mM)	X	mf	C_{CR} ($\times10^{-2}$mM)	n_2 ($\times10^{-12}m^2W^{-1}$)	$X_R^{(3)}$(m^3 W^{-1} s^{-1})	γ_R($\times10^{-23}$ $m^6W^{-1}s^{-1}$)
Toluene	0.5	5	0.005	0.03648	6.414	0.04885	5.56747
			0.008	0.05841	7.89	0.06009	4.27784
			0.01	0.07304	8.84	0.06733	3.8328
			0.02	0.14637	12.1	0.09216	2.61786
	0.5	10	0.001	0.01249	1.8	0.01371	4.5649
			0.002	0.02498	4.65	0.03542	5.8952
			0.004	0.04998	9.737	0.07416	6.16987
			0.006	0.07499	9.26	0.07053	3.91026
			0.008	0.10003	10.94	0.08332	3.46344

and

$$g = \frac{3}{2}\left[\frac{n^4-1}{(n^2+2)^2}\right] \quad (10)$$

In which, ε (permittivity) and n (the solvent of the refractive index) were the polarity of the sample. The parameters of p_1p_1 and p_2p_2 could be also found through the following equations:

$$p_1 = \frac{2(\mu_e-\mu_g)^2}{hca^3} \quad (11)$$

and

$$p_2 = \frac{2\left(\mu_e^2-\mu_g^2\right)}{hca^3} \quad (12)$$

Wherein; c (light velocity), h (Planck's constant), μ_e/μ_g (the ground state dipole moments), and μ_e/μ_g (the excited state dipole moments) were obtainable in Eqs. 11 and 12. The μ_e/μ_g could be also extracted from Eqs. 11 and 12 and the results were illustrated in Table 1. The μ_e/μ_g values of PpIX in water-ethanol was constant at 1.45 and the change of absorption and fluorescence peaks also depended on the dielectric constant of solutions.

In a previous study, the dipole moment of Crocin in solvent and microemulsion was studied using quantum mechanical perturbation theory [12] and the results indicated that the dipole moment of Crocin could change with microemulsion, while it was constant at different solvents. Thus, it was considered as a general effect in which the microemulsion could change the dipole moment of the dyes.

NLO Properties of PpIX

The normalized closed and open aperture curves of PpIX in water were presented in Fig. 3a, b. The results showed the depth of open aperture curves and the distance between the peak and the valley of close daperture curve growth as PpIX concentration increased (Fig. 3).

The β and n_2 values were also extracted based on Fig. 3 as along with Eqs. 2 and 6 and the results were presented in Fig. 4. The value of β and n_2 growth with the upsurge of PpIX concentration was due to the number of PpIX.

The NLO properties of the PpIX in AOT/Toluene/H_2O were studied using z-scan. The open aperture curve of AOT/Toluene/H_2O/PpIX was also examined at X = 5 (Fig. 5a) and X = 10 (Fig. 5b) for different mass fractions and the closed aperture curves of AOT/Toluene/H_2O/ PpIX were studied at X = 5 (Fig. 5c) and X = 10 (Fig. 5d) for different mass fractions. The value of β and n_2 extracted as well as the results were illustrated in Fig. 6. The value of β and n_2 did not depend on the molar ratio of AOT/Toluene/H_2O. Furthermore; the β and n_2 values in AOT/Toluene/H_2O at the constant dye concentration were greater than aqueous solutions, caused by the decrease of solvent polarity and reduction of PpIX aggregation in AOT/Toluene/H_2O.

According to the results, the PpIX aggregation in water was greater than microemulsion that could

Table 4 The σ_2 value of PpIX in water at different PpIX concentration

Solvent	C_{dye} (mM)	β ($\times10^{-7}$cmW^{-1})	*absorption Cross section* $\left(\times10^{-40}m.\frac{s}{lit}\right)$
Water	0.04	0.772	0.0119842
	0.06	2.59	0.026804
	0.075	5.043	0.0417522
	0.1	5.93	0.0368219

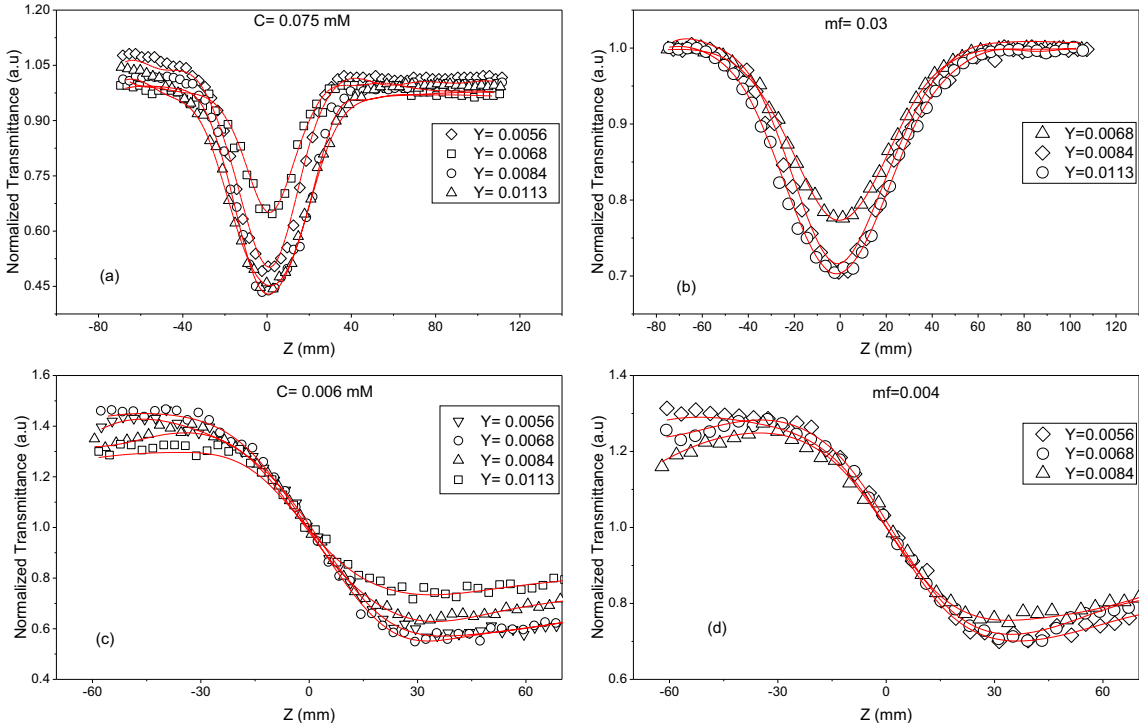

Fig. 7 The open aperture curve of (**a**) RPMI in water with PpIX/Water = 0.0 75 mM and (**b**) AOT/Toluene/H_2O/PpIX at mf = 0.075, X = 10 and PpIX/water = 0 .5mM. The close aperture curve of RPMI in (**c**) water and (**d**) AOT/Toluene/H_2O/PpIX at mf = 0.004, X = 10 and PpIX/water = 0 .5mM at different RPMI concentration in solution (Y)

decrease the μ_g of PpIX. The reduction of the μ_g of PpIX could also moderate the value of β and n_2.

In this respect, the third-order susceptibility (real part) could be defined via Eqs. 13 and 14 [20]:

$$\chi_R = 2n_2 n_0^2 \varepsilon_0^2 c \tag{13}$$

The hyperpolarizability (real part); γ_R, was signified by Eq. 14 [21].

$$\gamma_R = \frac{\chi_R}{L^4 N} \tag{14}$$

In which; L was the Lorenz parameter. The values of χ_R and γ_R of PpIX in the solutions were also extracted from the values of the n_2 (Figs. 4b and = 6c, d) as presented in Tables 1 and 2. There was also a descending trend for the γ_R values as the concentration upsurged. This was ascribed to the reality that the dipole moment of PpIX could change based on the concentration [18]. The nonlinear absorption cross-sections (σ_2) could be also labeled via Eq. 15 [22].

$$\sigma_2 = \frac{\beta E_\upsilon \times 10^3}{N C_{PpIX}} \tag{15}$$

Table 5 The nonlinear absorption cross-sections (σ_2) value of PpIX in AOT/Toluene/H_2O at X = 5 and 10 with PpIX/Water = 0 .5mM and different droplet mass fraction (mf)

Oil	PpIX/water ratios (mM)	X	mf	C_{CR} ($\times 10^{-2}$mM)	β ($\times 10^{-7}$mW^{-1})	*absorption Cross section* $\left(\times 10^{-40} m.\frac{s}{lit}\right)$
Toluene	0.5	5	0.04	0.293916	3.55	0.749992
			0.07	0.517486	5.26	0.63116
			0.09	0.668051	6.91	0.642274
	0.5	10	0.02	0.250639	1.438	0.356257
			0.025	0.313597	3.32	0.657382
			0.03	0.376676	5.139	0.847155
			0.04	0.503196	6.65	0.82061
			0.05	0.630201	6.96	0.685776

Table 6 The β and σ_2 values of water/PPIX with PpIX/water =0 .5mM at different RPMI concentration

Solvent	PpIX/water ratios (mM)	C_{dye} (mM)	RPMI/ water(Y)	β ($\times 10^{-7}$cmW^{-1})	*absorption Cross section* $\left(\times 10^{-40} m.\frac{s}{lit}\right)$
Water	0.5	0.075	0.0113	4.73	0.0391608
		0.075	0.0084	4.76	0.0394092
		0.075	0.0068	4.53	0.037505
		0.075	0.0056	3.8	0.0314611

Wherein, E is the energy of the laser and N shows Avogadro constant. According to Figs. 4a and 6a and Eq. 9, the value of σ_2 was extracted, as shown in Tables 3 and 4.

The σ_2 value of PpIX in AOT/Toluene/H_2O was greater than that of water. As mentioned before, the PpIX aggregation in AOT/Toluene/H_2O was lower than that in water which could enhance the value of σ_2. Moreover, the dielectric constant of AOT/Toluene/H_2O was reproted less than that of water which could change the value of the nonlinear absorption cross-sections.

Effect of Cell Culture Medium on PpIX

RPMI is a system used in cell culture. Normally, the RPMI can be used to study PTD in cell culture in a laboratory environment. In this study, the mixture of RPMI in water and AOT/Toluene/H_2O/PpIX was studied at different RPMI concentrations. Moreover, the open aperture curve of RPMI in water (Fig. 7a) and RPMI in AOT/Toluene/H_2O/PpIX at mf = 0.075, X = 10, and PpIX/water = 0 .5mM (Fig. 7b) were studied. The closed aperture curve of RPMI in water (Fig. 7c) and AOT/Toluene/H_2O/PpIX at mf = 0.004, X = 10, and PpIX/water = 0 .5mM (Fig. 7d) were also considered. The β and σ_2 values of water/PpIX and AOT/Toluene/H_2O/PpIX at X = 10 and mf = 0.03 and PpIX/Water = 0 .5mM at a different RPMI concentration were similarly extracted from Fig. 7a, b and the results were outlined in Tables 5 and 6. Moreover, the β and σ_2 values upsurged with the increase in PRMI concentration in solutions.

The values of n_2, χ_R, and γ_R of water/PpIX and AOT/Toluene/H_2O/PpIX at X = 10 and mf = 0.004 and PpIX/Water = 0 .5mM at a different RPMI concentration were also extracted from Fig. 7c, d and the results were illustrated in Tables 7, 8, and 9. There was also a growth in β and σ_2 values as the PRMI concentration in solutions increaaed. According to the results of this study, the reduction of PpIX aggregation in solutions could increase the NLO properties. Thus, the increase of RPMI concentration in water and microemulsion could reduce PpIX aggregation in solutions.

PCS of AOT/Toluene/H_2O/PpIX

PCS was used to find the effect of PpIX on the nano-confined water of AOT/Toluene/H_2O. The light source of PCS was He-Ne laser and the scattering angle was $\alpha = 90^0$. The q was also determined by Eq. 16 [23, 24].

$$q = \frac{4\pi n}{\lambda}\sin\left(\frac{\theta}{2}\right) \tag{16}$$

In this formula; λ is the wavelength of the laser and θ shows the angle of scattering. In PCS, the second-order autocorrelation function $g_2(\tau)$ could be specified via Eq. 17:

$$g_2(\tau) = \frac{\langle I(t)I(t+\tau)\rangle}{\langle I(t)\rangle^2} \tag{17}$$

Wherein, τ refers to the correlation time. The function $g_1(t)$ was also connected to the first-order correlation function $g_1(t)$ through the Siegert relation [22].

$$g_2(\tau) = 1 + P|g_1(\tau)|^2 = 1 + P\exp(-2t/\tau) \tag{18}$$

Table 7 The β and σ_2 values of AOT/Toluene/H_2O/PpIX at X = 10 and mf = 0.03 and PpIX/Water = 0 .5mM at different RPMI concentration

Microemulsion	RPMI/ water(Y)	β ($\times 10^{-7}$cmW^{-1})	*Nonlinear absorption Cross section* $\left(\times 10^{-40} m.\frac{s}{lit}\right)$
PpIX/water ratios (mM) = 0.5 X = 10 mf = 0.03	0.0113	2.64	78.0614
	0.0084	2.39	70.6693
	0.0068	1.9	56.1806

Table 8 The values of n_2 and χ_R, γ_R of water/PPIX at different RPMI concentration

Solvent	PpIX/water ratios (mM)	C_{dye} (mM)	RPMI/water (Y)	$n_2(\times10^{-12}$ m^2 W$^{-1})$	$X_R^{(3)}$(m^3 W^{-1} s^{-1})	$\gamma_R(\times10^{-20}\ m^6W^{-1}s^{-1})$
Water	0.5	0.006	0.0113	3.85	26.15142	0.290549
		0.006	0.0084	5.61	38.10635	0.423372
		0.006	0.0068	5.97	40.55168	0.45054
		0.006	0.0056	6.11	41.50264	0.461105

Table 9 The values of n_2 and χ_R, γ_R of AOT/Toluene/H_2O/PpIX at X = 10 and mf = 0.004 and PpIX/Water = 0 .5mM at different RPMI concentration

Microemulsion	RPMI/water (Y)	n_2 $(\times10^{-12}$m^{2}W$^{-1})$	$X_R^{(3)}$(m^3 W^{-1} s^{-1})	$\gamma_R(\times10^{-20}\ m^6W^{-1}s^{-1})$
PpIX/water ratios (mM) = 0.5X = 10mf = 0.004 C_{dye} $(\times10^{-2}$mM)= 0.04998	0.0084	3.65	0.0278	0.412801
	0.0068	4.1	0.03123	0.463695
	0.0056	4.41	0.03359	0.498754

In which, the collective diffusion coefficient could be extracted from the following equation:

$$D_c = \frac{1}{q^2\tau} \tag{19}$$

The autocorrelation function of AOT/Toluene/H_2O with and without PpIX at a constant X = 10, mf = 0.07, and three different dye/water = 0, 0.2 and 0 .5mM were also studied and the outcomes were presented in Fig. 8. With the increase in the dye/water ratio, the second peak of autocorrelation function was illustrated in Fig. 8. The second peak could be because of the dye-droplet aggregation in AOT/Toluene/H_2O.

The size of water-droplet of AOT/Toluene/H_2O with X = 10 and mf = 0.07 was extracted at 4 .9nm and that in the AOT/Toluene/H_2O/PpIX with X = 10, mf = 0.07, and dye/water = 0.2 two different sizes were also extracted at 5.1 and 225 nm using PCS. These results indicated that the dye-droplet aggregation had increased by the upsurge of dye concentration. In a previous study, the PCS of the Rhodamine 6G with n-Decane/AOT/H_2O had been studied [16] and the results had revealed that the size of AOT nano-droplets could be affected by R6G/water concentration in the water/AOT/n-decane system. In the present case, the size of AOT/Toluene/H_2O also changed as PpIX concentration increased.

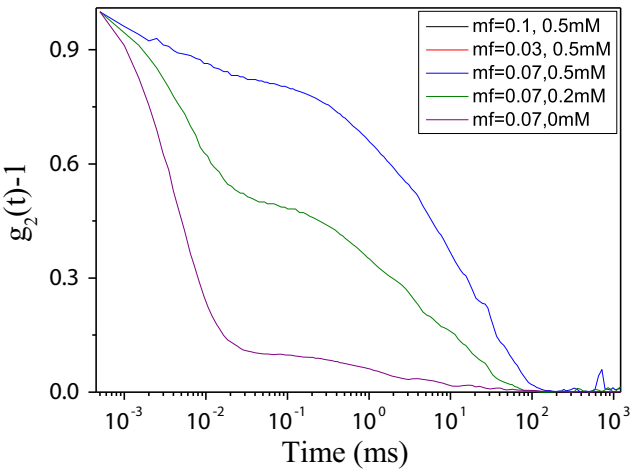

Fig. 8 The autocorrelation function of PpIX in AOT/H_2O/ Toluene at X = 10 and three mass fraction at three different dye/water = 0, 0.2, 0 .5mM

Conclusion

The effect of solvent polarity, surfactant interaction, microemulsion, and cell cultural medium on absorbance, fluorescence, and NLO properties of PpIX was examined in this study. In this resepct, reduction of solvent polarity induced a blueshift in absorbance and a redshift in fluorescence spectra of PpIX. The β and n_2 values of PpIX in water and water-ethanol were also studied and the results were compared with those for microemulsion. The findings indicated that β and n2 values had enhanced in microemulsion compared with other solvents, owing to polarity reduction as well as interaction of surfactant with PpIX. The effect of cell culture medium (i.e. RPMI) on NLO properties of PpIX was also examined. The β value increased following growth in RPMI concentration in microemulsion and aqueous solutions. According to the results of PCS, a growth was observed in dye-droplet aggregation following a rise in PpIX concentration in micoremulsion.

References

1. Imanparast A, Bakhshizadeh M, Salek R, Sazgarnia A (2018) Pegylated hollow gold-mitoxantrone nanoparticles combining photodynamic therapy and chemotherapy of cancer cells. Photodiagn Photodyn Ther 23:295–305
2. Xin,Wang Xue Yin, Xiao-Yong Lai, Ying-Tao Liu (2018) A theoretical study of a series of water-soluble triphenylamine photosensitizers for two-photon photodynamic therapy. Spectrochim Acta A 203: 229–235
3. Liu Y-T, Li Y-R, Wang X, Bai F-Q (2017) Theoretical investigation of NˆCˆN-coordinated Pt(II) and Pd(II) complexes for long-lived two-photon photodynamic therapy. Dyes Pigments 142:55–61
4. Liu B, Wang J, Wang X, Liu B-M, Kong Y-M, Wang D, Xu S-K (2010) Spectrometric studies on the Sonodynamic damage of protein in the presence of levofloxacin. J Fluoresc 20(5):985–992
5. Goyan RL, Cramb DT (2000) Near-infrared two-photon excitation of Protoporphyrin IX: Photodynamics and photoproduct generation. Photochem Photobiol 72(6):821–827
6. Flávia R. O. Silva, Camila T. Nabeshima, Maria H. Bellini, Nestor Schor, Nilson D. Vieira Jr, Lilia C. Courrol (2013) Study of ProtoPorphyrin IX elimination by body excreta: a new noninvasive Cancer diagnostic method? J Fluoresc, 23(1):131–135
7. Scolaro LM, Castriciano M, Romeo A, Patane S, Cefalı E, Allegrini M (2002) Aggregation behavior of Protoporphyrin IX in aqueous solutions: clear evidence of vesicle formation. J Phys Chem B 106: 2453–2459
8. Jafari A, Naderali R, Motiei H (2017) The effect of doping acid on the third-order nonlinearity of carboxymethyl cellulose by the Z-scan technique. Opt Mater 64:345–350
9. Wang K, Ju Y, He J, Zhang L, Chen Y, Blau WJ, Wang J (2014) Nonlinear optical propagation in a tandem structure comprising nonlinear absorption and scattering materials. Appl Phys Lett 104: 021110
10. Hu W, He T, Jiang R, Yin J, Li L, Lu X, Zhao H, Zhang L, Huang L, Sun H, Huang W, Fan Q (2017) Inner salt-shaped small molecular photosensitizer with extremely enhanced two-photon absorption for mitochondrial-targeted photodynamic therapy. Chem Commun 53: 1680–1683
11. Sangsefedi SA, Sharifi S, Rezaion HRM, Azarpour A (2018) Fluorescence and nonlinear optical properties of alizarin red S in solvents and droplet. J Fluoresc 28(3):815–825
12. Azarpour A, Sharifi S, Rakhshanizadeh F (2018) Nonlinear optical properties of Crocin: from bulk solvent to Nano-confined droplet. J Mol Liq 252:279–288
13. Zakerhamidi SMS (2017) Third order nonlinear responses of basic blue 55 molecules in polar solvents. Optik 130:743–749
14. Khadem Khadije Vahedi M, sharifi s, Alizadeh K, Marti O, Amirkhani M (2018) Enhancement of nonlinear optical response and fluorescence spectra of cationic neutral red by anionic surfactant. Opt Quant Electron 50(24):1–17
15. Gayathri C, Ramalingam A (2007) Single-beam Z-scan measurement of the third-order optical nonlinearities of azo dyes. Spectrochim Acta A Mol Biomol Spectrosc 68:578–582
16. Pourtabrizi M, Shahtahmassebi N, Kompany A, Sharifi S (2018) Effect of microemulsion structure on fluorescence and nonlinear optical properties of rhodamine 6G. J Fluoresc 28(1):323–336
17. Sharifi S, Alizadeh K, Shavakandi SM (2018) Comments on "Photophysics of rhodamine B in the nanosized water droplets: a concentration dependence study". J.Mol.Liq. 247:467–469
18. Peyghami S, Sharifi S, Rakhshanizadeh F, Alizadeh K (2017) Nonlinear optical properties of rose Bengal: effect of environment. J Mol Liq 246:157–165
19. Shavakandi SM, Alizadeh K, Sharifi S, Marti O, Amirkhani M (2017) Optical study of xanthene type dyes in nano-confined liquid. J Phys D 50(15):155301
20. Bhushan B, Kundu T, Singh BP (2013) Nonlinear optical properties of two different Nanoassemblies of Polydiacetylene (PDA): PDA Nanovesicles and PDA nanocrystals. Optics and Photonics Journal 3:278–286
21. Bogdan E, Plaquet A'l, Antonov L, Rodriguez V, Ducasse L, Champagne B, Castet F (2010) Solvent effects on the second-order nonlinear optical responses in the keto-enol equilibrium of a 2-Hydroxy-1-naphthaldehyde derivative. J Phys Chem C 114: 12760–12768
22. Wielgus M, Bartkowiak W, Samoc M (2012) Two-photon solvatochromism. I. Solvent effects on two-photon absorption cross section of 4-dimethylamino-40-nitrostilbene (DANS). Chem Phys Lett 554:113–116
23. Sharifi S (2015) Relationship between relaxation processes of light scattering in network of droplets. Opt Spectrosc 118(2):317–323
24. Sharifi S, Nasrollahi A (2015) Effect of Dipalmitoylphosphatidylcholine on a microemulsion. Opt Spectrosc 118(6):893–898